Impact of a nearby subhalo on the constraint of dark matter annihilation from cosmic ray antiprotons*

Yi Zhao (赵熠)[1] Xiao-Jun Bi (毕效军)[2,3] Su-Jie Lin (林苏杰)[4] Peng-Fei Yin (殷鹏飞)[2†]

[1]College of Physics and Materials Science, Tianjin Normal University, Tianjin 300387, China
[2]Key Laboratory of Particle Astrophysics, Institute of High Energy Physics, Chinese Academy of Sciences, Beijing 100049, China
[3]School of Physical Sciences, University of Chinese Academy of Sciences, Beijing 100049, China
[4]Zhuhai Campus of Sun Yat-Sen University, Sun Yat-Sen University, Zhuhai 519082, China

Abstract: Numerous simulations indicate that a large number of subhalos should be hosted by the Milky Way. The potential existence of a nearby subhalo could have important implications for our understanding of dark matter (DM) annihilation. In this study, we investigate the hypothetical presence of a nearby subhalo and set the upper limits on the DM annihilation cross section by analyzing the cosmic-ray antiproton spectrum. By presenting the ratios of annihilation cross section limits for scenarios with and without a nearby subhalo, we can quantitatively evaluate the potential impact of the nearby subhalo on the limits of the DM annihilation cross section. The impacts of the concentration model and the subhalo probability distribution have been considered. We explore the antiproton contribution of the potential nearby DM subhalo accounting for the DAMPE $e^{\pm}$ spectrum at ~ 1.4 TeV and find that the current AMS-02 antiproton results do not limit this contribution.

Keywords: dark matter, antiproton, subhalo

DOI: 10.1088/1674-1137/ad13f7

I. INTRODUCTION

The nature of dark matter (DM) remains one of the most pressing questions in modern astrophysics, cosmology, and particle physics. In the standard cosmology scenario, the formation of luminous galaxies occurs within the halos of cold and collisionless non-baryonic DM. Traditionally, the DM distribution has been modeled as a smoothly distributed component with a spherically symmetric density profile, such as an isothermal or Navarro-Frenk-White (NFW) profile [1]. However, a large number of theoretical arguments suggest that the DM distribution in galactic halos may exhibit significant substructures [2−18].

DM halos are thought to form through gravitational amplification of initial fluctuations in a bottom-up manner, in which smaller objects collapse and merge into larger ones over time. Extensive N-body simulations have revealed that some of the total halo mass can endure tidal disruption, appearing as distinct subhalos within host halos. [4, 19−23]. The existence of subhalos in galactic halos has been confirmed through numerous high-resolution numerical simulations. This is a key aspect of the standard cosmology with hierarchical structure formation.

Simulations indicate that the Milky Way should host hundreds of subhalos [4, 24−28]. However, astrophysical mechanisms suggest that many subhalos are challenging to observe as they are non-luminous and not very massive. The number of satellite galaxies observed around the Milky Way is smaller than the projected number of DM subhaloes predicted by the cold DM model. This suggests the existence of a substantial quantity of exceedingly dim galaxies and DM-dominated haloes with minimal or negligible stellar content within the Local Group.

If the DM particles exist as weakly interacting particles, which are well-motivated DM candidates, subhalos can be traced through the products resulting from DM annihilation. They can boost the fluxes of annihilation products, potentially enabling their detection in cosmic ray observations. Such observations offer a unique avenue for exploring the particle properties of DM and could provide insights into the DM structure.

The study of antimatter particles is particularly significant in this field. The accurate quantification of antiproton spectra by space-borne instruments like AMS-02 offers excellent sensitivity to probe DM particles. These antiprotons are expected to primarily originate from inelastic collisions between cosmic rays and the interstellar medium. However, they may also be generated through DM

Received 9 November 2023; Accepted 11 December 2023; Published online 12 December 2023

* Supported by the Science & Technology Development Fund of Tianjin Education Commission for Higher Education (2020KJ003).

† E-mail: yinpf@ihep.ac.cn

annihilation or decay. For example, the tentative excess at $O(10)$ GeV of the AMS-02 antiproton data can be explained by DM annihilation [29, 30]. Various discussions on this issue can be found in the literature [31−39].

In this study, we specifically examine the impact of the possible nearby subhalo on antiprotons induced by DM annihilation. The constraints on the thermally averaged annihilation cross section of DM $\langle\sigma v\rangle$ are investigated using the antiproton spectra measured by AMS-02 [40]. Subsequently, we propose the hypothesis that a DM subhalo of a certain mass and distance from the Earth exists and investigate how such a subhalo influences the limits on $\langle\sigma v\rangle$. Meanwhile, we examine how the concentration model and potential subhalo distribution could impact this study individually. We also explore the antiproton limits for the potential nearby DM subhalo accounting for the DAMPE $e^{\pm}$ spectrum at ~ 1.4 TeV [41].

This paper is organized as follows. In Sec. II, we briefly introduce the calculation of the antiprotons from the cosmic ray interactions and the smooth DM component. In Sec. III, we set the constraints on the DM $\langle\sigma v\rangle$ with the contribution from the nearby DM subhalo. The contribution from a series of DM subhalos is also discussed. In Sec. IV, we investigate the antiproton limits for the potential nearby DM subhalo accounting for the DAMPE $e^{\pm}$ spectrum at ~ 1.4 TeV. Finally, Sec. V is the conclusion.

II. ANTIPROTONS FROM COSMIC RAY INTERACTIONS AND THE SMOOTH DM COMPONENT

In this work, we utilize the numerical tool GALPROP [42, 43] to derive the contribution of antiprotons from the cosmic ray interactions and the smooth DM component. The propagation of cosmic rays in the Milky Way can be characterized by the diffusive transport equation [44], which includes the following primary propagation parameters: diffusion coefficient at the reference rigidity D_0, diffusion coefficient index δ, Alfvenic speed v_A for reacceleration purposes, half-height of the propagation halo z_h, assumed broken power-law in rigidity with indices ν_1 and ν_2 below or above the break rigidity R_{br} for the injection spectrum of cosmic-ray nuclei, and propagated flux normalization of protons A_p. As the DM contributions are involved, the assumptions of the DM mass, thermally averaged annihilation cross section, annihilation channel, and density profile are also required. For the solar modulation effect, we consider the simple force field model with one parameter of the modulation potential Φ.

We find that the diffusion-reacceleration propagation model is better than the diffusion-convection model when fitting the antiproton flux measured by AMS-02, as has been previously reported [30, 45]. Therefore, we adopt the diffusion-reacceleration propagation model in this work. For the main propagation parameters, we take the values $D_0 = 7.24\times10^{28}\ \mathrm{cm^2\cdot s^{-1}}$, $\delta = 0.38$, $v_A = 38.5\ \mathrm{km\cdot s^{-1}}$, $z_h = 5.93$ kpc, $\nu_1 = 1.69$, $\nu_2 = 2.37$, $\log_{10}(R_{br}) = 4.11$, and $\log_{10}(A_p) = -8.347$, which are obtained from the Markov Chain Monte Carlo fit in Ref. [45]. Afterward, we free the solar modulation Φ in the range of (0.3, 0.8) GV. We also add an energy-independent rescaling factor κ for the secondary antiproton flux in the fit, which is used to describe the uncertainty of the antiproton production cross sections in proton-proton collisions [46]. This factor is allowed to vary within (0.5, 2.0) in the fit but is approximately equal to 1 for the best-fit results. The DM density distribution is adopted to be the NFW profile [1]

$$\rho(r) = \frac{\rho_s}{(r/r_s)(1+r/r_s)^2}. \tag{1}$$

For the Galactic halo, we take $\rho_s = 0.35\ \mathrm{GeV\cdot cm^{-3}}$ and $r_s = 20$ kpc, which correspond to a local DM density of $0.4\ \mathrm{GeV\cdot cm^{-3}}$ near the solar system.

In Fig. 1, we take DM with a mass of 75 GeV as an example to show the antiproton prediction, comparing with the latest AMS-02 results [40]. We find that the experimental data can be well fitted by the antiprotons from cosmic-ray interactions, except that the antiproton flux at $O(10)$ GeV is potentially compensated by DM annihilation. Note that the significance of the antiproton excess at $O(10)$ GeV and corresponding DM interpretation depends on many complicated factors, such as the secondary antiproton production process, propagation, solar modulation, and unclear experimental correlated errors [31−39]. In this work, we focus on the impact of the nearby DM subhalo on the DM constraints and do not discuss this antiproton excess and the corresponding DM

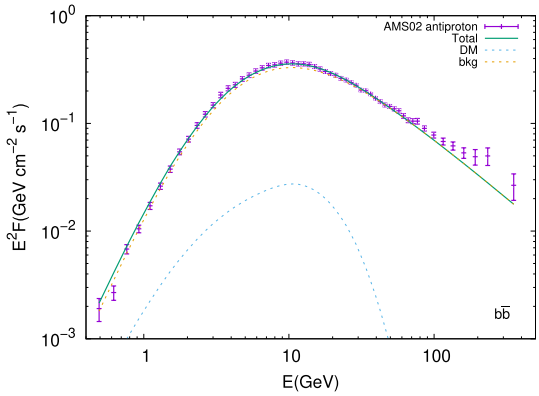

Fig. 1. (color online) The total antiproton flux (green solid line), comprised of the secondary antiprotons (orange dashed line) and those generated by DM annihilation (blue dashed line). The DM mass and $\langle\sigma v\rangle$ are 75 GeV and 0.9×10^{-26} $\mathrm{cm^3 s^{-1}}$, respectively.

interpretation.

III. DM ANNIHILATING TO $\bar{p}$ WITH THE NEARBY SUBHALO

In this section, we consider the DM contribution to antiprotons from the nearby subhalo, aiming to understand the extent of the impact of the nearby subhalo on the constraint of the DM $\langle\sigma v\rangle$. We take the nearby subhalo as an extended source and calculate its flux as

$$\phi^{r,E} = \int_0^{\pi} 2\pi \sin\theta \mathrm{d}\theta \int_0^{\infty} \phi_c^{r,E}(r',\theta) r'^2 \mathrm{d}r', \tag{2}$$

with

$$\phi_c^{r,E}(r',\theta) = \rho^2 \frac{\mathrm{d}N}{\mathrm{d}E} \frac{\langle\sigma v\rangle}{4m_\chi^2} C(d), \tag{3}$$

where r' is the distance from the halo center to the site of DM annihilation, r is the distance from the subhalo center to the Earth, θ is the angle between $\vec{r}$ and $\vec{r}'$, $\langle\sigma v\rangle$ is the thermally averaged DM annihilation cross section, $\mathrm{d}N/\mathrm{d}E$ is the initial DM annihilation spectrum obtained by PPPC [47, 48], m_χ is the DM mass, and ρ is the DM density. The propagation term $C(d)$ is given by

$$C(d) = \int_0^{\infty} \frac{1}{(4\pi D\tau)^{\frac{3}{2}}} \mathrm{e}^{-\frac{d^2}{4D\tau}} \mathrm{d}\tau, \tag{4}$$

where D is the diffusion coefficient, τ is the time interval between the emission time and observation time of the cosmic ray particle, and $d = \sqrt{r^2 + r'^2 - 2rr'\cos\theta}$ is the distance from the Earth to the position where DM particles annihilate.

The density profile of subhalos within the solar neighborhood demonstrated a suitable correspondence with the NFW profile, as obtained from high-resolution N-body simulation results [26]. Consequently, we employ the NFW profile to represent the DM density within the subhalo and determine the subhalo mass using the concentration model and parameters r_s and ρ_s in the NFW profile.

The concentration parameter is defined as the ratio of the virial radius to the scale radius of the halo $C = r_v/r_s$. This parameter describes the shape of the DM halo, offering a nuanced understanding of how DM is distributed throughout the cosmic structure. The concentration model can greatly influence the gravitational effects and interactions within galaxies and clusters. It depends on the mass and formation history of the halo and is typically determined from numerical simulations of structure formation. Here, we adopt the concentration model in Ref. [49] (referred to as model 1), which is an approximation for the solar neighborhood based on the results of the N-body simulation Aquarius [26]. The concentration parameter C is determined by the relation

$$8.66\times10^6 \left(\frac{M_{\rm sub}}{10^6 M_\odot}\right)^{-0.18} = \frac{200}{3} \frac{C^3}{\ln(1+C) - \frac{C}{(1+C)}}, \tag{5}$$

where $M_{\rm sub}$ is the mass of subhalo and $M_\odot$ is the solar mass.

In this work, we use the latest AMS-02 antiproton result [40] to set the 95% C.L. upper limits on the DM $\langle\sigma v\rangle$. The mass of nearby subhalo is considered in the range of $10^6 - 10^9 M_\odot$. To enable a comparison, we adopt the same set of propagation parameters in all calculations, but Φ and κ are left to be free. In Figs. 2 (a) and (b), we illustrate the resulting limits on $\langle\sigma v\rangle$ for the $b\bar{b}$ channel with subhalo distances of 0.3 kpc and 1 kpc, respectively. We present the results as a ratio of 3×10^{-26} cm^{3}s^{-1}, which is the so-called natural value corresponding to the correct DM relic density from thermal production. For a certain DM mass, the $\langle\sigma v\rangle$ limits vary indistinctively with the change of subhalo mass.

We present the ratios of the limits on $\langle\sigma v\rangle$ in the scenarios with and without the nearby subhalo at distances of 0.3 kpc and 1 kpc in Figs. 2 (c) and (d), respectively. The existence of a nearby subhalo makes the limits more stringent. Consequently, the values of the ratios in Figs. 2 (c) and (d) are less than 1. In Fig. 2 (c), the limits are minimally influenced by the subhalo masses below approximately $10^6 M_\odot \sim 10^7 M_\odot$ at a distance of 0.3 kpc, as depicted by the blue regions. The subhalo masses up to about $10^8 M_\odot \sim 10^9 M_\odot$ have a significant impact on the limits, as shown by the yellow to red regions. The value of the deepest red region in Fig. 2 (c) indicates that the limits on the DM $\langle\sigma v\rangle$ with a subhalo are about one order of magnitude lower than the limits without a subhalo. A subhalo at a greater distance of 1 kpc leads to a weaker constraint on the DM $\langle\sigma v\rangle$ than that at a distance of 0.3 kpc, and its presence also has a less pronounced impact on the limits.

We also present the limits on $\langle\sigma v\rangle$ for the $b\bar{b}$ channel at 95% C.L., with respect to various subhalo distances and masses. The limits as a ratio of 3×10^{-26} cm^{3}s^{-1} for two DM masses of 75 GeV and 1 TeV are displayed in Figs. 3 (a) and (b), respectively. We can see that for a given distance, the differences in the $\langle\sigma v\rangle$ limits corresponding to different subhalo masses increase as the DM mass increases. The ratios of $\langle\sigma v\rangle$ limits for the scenarios with and without the nearby subhalo for DM masses of 75 GeV and 1 TeV are presented in Figs. 3 (c) and (d), respectively. As shown in Fig. 3 (c) or (d). When the hypothetical subhalo mass is below $\sim 10^7 M_\odot$ in the blue region, the presence or absence of the subhalo has a minor effect on the $\langle\sigma v\rangle$ limits. However, in the red region, the

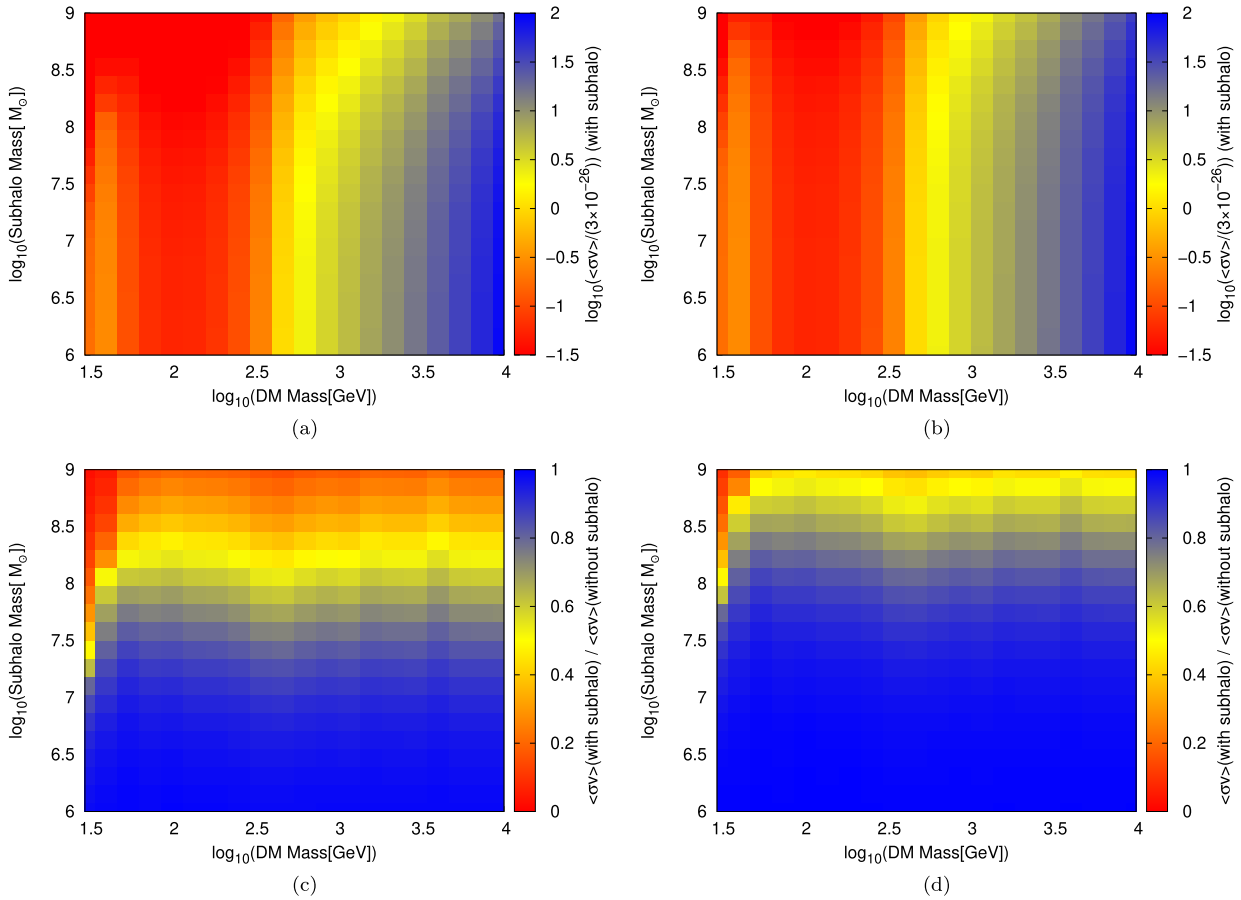

Fig. 2. (color online) The upper limits on $\langle\sigma v\rangle$ for the $b\bar{b}$ channel at 95% C.L. with the contribution from the nearby subhalo at distances of 0.3 kpc (a) and 1 kpc (b) from the subhalo are shown in panels (a) and (b), respectively. The ratios of $\langle\sigma v\rangle$ limits for the scenarios with and without the nearby subhalo at distances of 0.3 kpc and 1 kpc are displayed in panels (c) and (d), respectively.

existence of a subhalo would affect the limits considerably, with a maximum impact of approximately one order of magnitude. The DM mass does not have a significant impact on this result. The ratio of the $\langle\sigma v\rangle$ limits for the DM mass of 75 GeV is similar to that for 1 TeV, as shown in Figs. 3 (c) and (d), respectively.

$b\bar{b}$ and W^+W^- are two typical channels for the antiproton signals from DM. The constraints on $\langle\sigma v\rangle$ for the W^+W^- channel are also investigated. We find that for various subhalo distances and masses, the limits are comparable to those of the $b\bar{b}$ annihilation channel with minor differences, owing to the similar initial contributions of these two channels.

In Ref. [50], the probability distribution has been provided for finding a particular subhalo with the given annihilation luminosity $\mathcal{L} = \int \rho^2 \mathrm{d}V$ and distance, which is inferred from the N-body simulation Via Lactea II [27]. Using this result, we show the probabilities of 0.1% and 1% for finding a particular subhalo as the black solid and dashed lines in Fig. 3, respectively.

Considering the impact of the concentration model, we utilize an alternative model for comparison (referred to as model 2) provided by Ref. [51]

$$\log C = 0.971 - 0.094 \log \frac{M_{\rm sub}}{10^{12} M_\odot}. \tag{6}$$

Taking the subhalo distance as 0.3 kpc, we present the same analysis as Fig. 2 (c) in Fig. 4. Compared with the results in Fig. 2 (c), Fig. 4 exhibits no red region where the nearby subhalo could significantly affect the constraints. This indicates that the presence of a subhalo with lower concentration has a relatively smaller impact on the constraints of the DM $\langle\sigma v\rangle$. It is not strange that the concentration parameter significantly impacts the results since it determines the shape of the subhalo. The concentration in model 2 is smaller than that in model 1 for the same subhalo mass. A smaller concentration implies that the material distribution within this subhalo is relatively scattered, with a relatively larger core. Such subhalos may have undergone more interactions and merging events during their formation and evolution, leading to a less centralized distribution of matter. They would contribute less to cosmic rays owing to smoother density pro-

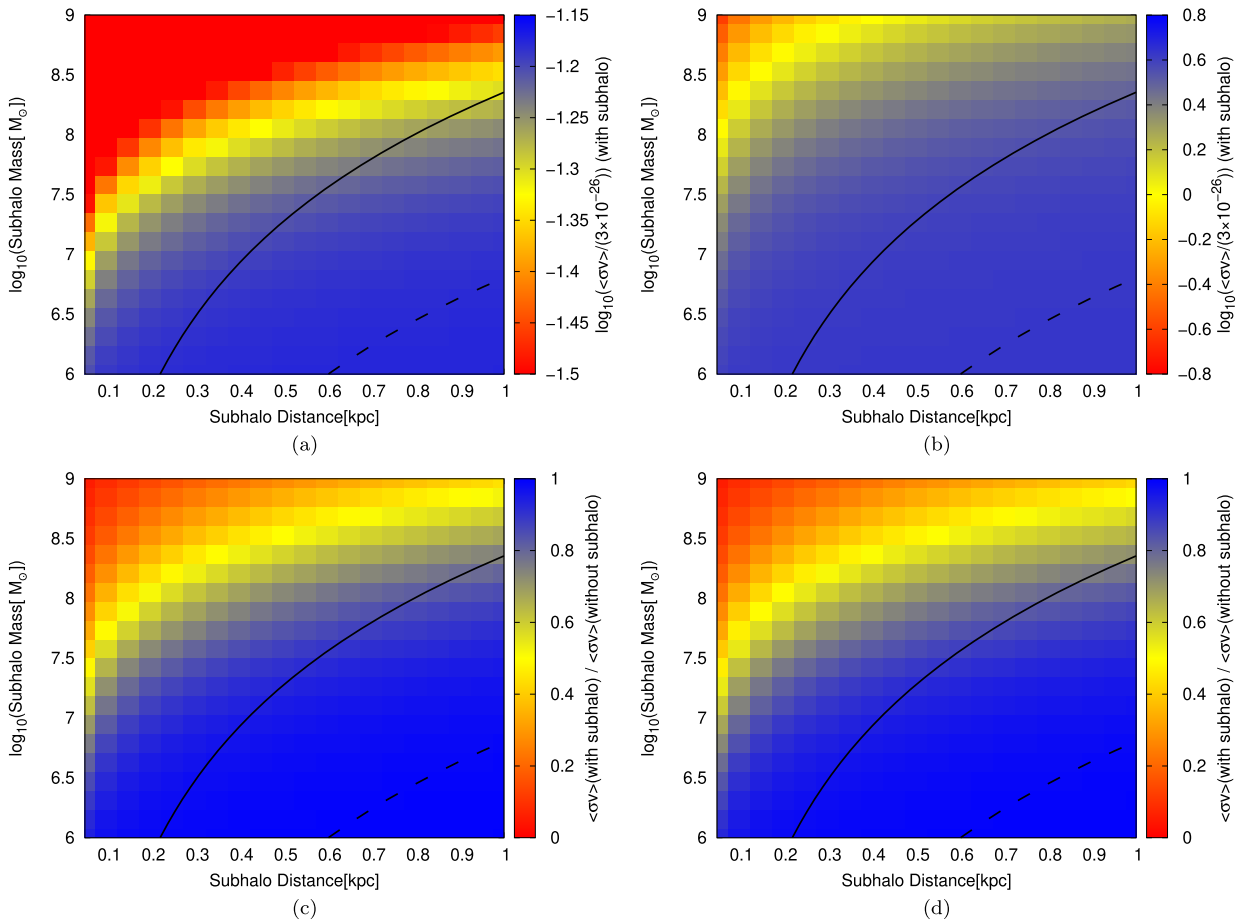

Fig. 3. (color online) The upper limits on $\langle\sigma v\rangle$ for the $b\bar{b}$ channel at 95% C.L. for the DM masses 75 GeV and 1 TeV are shown in panels (a) and (b), respectively. The ratios of the $\langle\sigma v\rangle$ limits for the scenarios with and without the nearby subhalo for the DM masses 75 GeV and 1 TeV are shown in panels (c) and (d), respectively. The solid and dashed lines indicate that the probabilities of finding a subhalo with the specific mass and distance are 0.1% and 1%, respectively.

files.

A single nearby subhalo is assumed in the above analysis. The existence of a wealth of subhalos would further enhance the DM annihilation flux compared with the smooth DM distribution. This enhancement is often described by the boost factor, which is defined as the ratio of the annihilation luminosity, including the subhalo contribution, to that originating from the smooth DM component. The boost factor at a galactocentric radius r can be given by

$$B(r) = \frac{\int \rho^2 \mathrm{d}V}{\int \bar{\rho}^2 \mathrm{d}V} = \int_0^{\rho_{\max}} P(\rho, r)\frac{\rho^2}{\bar{\rho}^2}\mathrm{d}\rho, \tag{7}$$

where $\bar{\rho}$ is the mean density, which is roughly equal to the smooth DM density, and $P(\rho, r)$ is the probability distribution that the particular position at r has the density ρ.

With the $P(\rho, r)$ determined by N-body simulations, the boost factor can be further given by [52, 53]

$$B(r) = f_s \mathrm{e}^{\Delta^2} + (1 - f_s)\frac{1+\alpha}{1-\alpha}\left[\left(\frac{\rho_{\max}}{\rho_h}\right)^{1-\alpha} - 1\right], \tag{8}$$

where $f_s \sim 1$ is the fraction of the smooth component in the DM density, and ρ_h is the smooth DM density distribution. The first term resulting from the finite width Δ of the smooth density is roughly equal to 1 due to small Δ. The second term comes from the contribution of subhalos. The analysis of Ref. [52] shows that $f_s(r)$, α, and $\rho_{\max}$ can be taken as $1 - 7\times10^{-3}[\bar{\rho}(r)/\bar{\rho}(r = 100\ \mathrm{kpc})]^{-0.26}$, 0, and 80 GeV $\cdot$ cm^{-3}, respectively.

Taking the DM masses of 75 GeV and 1 TeV as examples, we conduct the same analysis as shown in Fig. 3. Specifically, we derive the upper limits on the DM $\langle\sigma v\rangle$ in the presence of subhalos, and the ratio of the upper limits on the DM $\langle\sigma v\rangle$ with and without subhalos. When investigating the impact of subhalos, the contributions from the single nearby subhalo and a series of subhalos

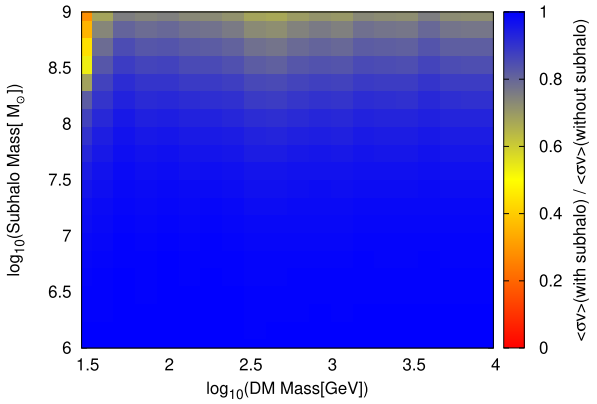

Fig. 4. (color online) The same as Fig. 2 (c), except that concentration model 2 is considered here.

are considered. The results reveal that the upper limits on $\langle\sigma v\rangle$ with the contribution from a series of subhalos is slightly stricter than that without such contribution by a factor of $\sim 0.8-0.9$.

At the end of this section, we give a brief comment on the anisotropy resulting from the nearby subhalo. It can be expected that the nearby cosmic ray source induces an anisotropy along its direction, which can be estimated as $3D|\nabla f|/cf$, where f is the local cosmic ray flux. For the nearby subhalo considered here, this anisotropy can be roughly estimated as $\sim Df_{\rm sig}/crf_{\rm bkg}$, and is suppressed by the ratio of the signal flux from the source to the background flux $f_{\rm sig}/f_{\rm bkg}$. However, a large experimental statistic will be required to detect such anisotropy.

IV. DM ANNIHILATION TO $e^{\pm}$ AND $\bar{p}$ WITH THE NEARBY SUBHALO

The aforementioned findings have practical implications for the following discussion. The DAMPE collaboration reported the measurement of the overall spectrum of electrons and positrons ranging from tens of GeV to several TeV, which revealed a tentative peak structure at around 1.4 TeV [54]. High energy electrons and positrons at ~TeV cannot travel long distances in the Milky Way owing to the strong cooling effect resulting from synchrotron radiation and inverse Compton scattering. A favored hypothesis to explain this sharp spectral structure is a monochromatic injection of $e^{\pm}$. However, the astrophysical source cannot directly generate such a monochromatic flux, and the required source should be young and close to Earth. On the other hand, DM annihilation in a nearby subhalo may be a promising explanation for this tentative sharp structure [49].

We employ a similar approach to produce the peak feature in the $e^{\pm}$ spectrum. To account for the DM contribution to $e^{\pm}$, we should consider the rate of energy loss for $e^{\pm}$ in propagation. This rate is approximated as

$$-\frac{{\rm d}E}{{\rm d}t} \equiv b(E) = b_0 + b_1\frac{E}{1{\rm GeV}} + b_2\left(\frac{E}{1{\rm GeV}}\right)^2, \quad (9)$$

where $b_0 \approx 3\times10^{-16}$ GeV/s and $b_1 \approx 10^{-15}$ GeV/s represent the rates of energy loss caused by the ionization and bremsstrahlung processes in neutral gas with a density of 1 cm^{-3}, respectively, and $b_2 \approx 10^{-16}$ GeV/s represents the rate of energy loss caused by the synchrotron and inverse Compton scattering processes. The total energy density of the magnetic field and interstellar radiation field is assumed to be 1 eV/cm^3.

We compute the $e^{\pm}$ spectrum resulting from DM with a mass of 1.5 TeV through the e^+e^- channel for a range of assumed subhalo masses and distances. The subhalo mass and distance are taken from $10^6-10^9M_\odot$ and $0.05-0.5$ kpc, respectively. Then we obtain the best fit $\langle\sigma v\rangle_{e^{\pm}}$ accounting for the tentative sharp structure in the DAMPE $e^{\pm}$ spectrum.

Meanwhile, we utilize the antiproton spectrum observed by AMS-02 to constrain the DM $\langle\sigma v\rangle$ for such nearby subhalo. Although the leptonic channels do not directly produce antiprotons, the gauge bosons originating from annihilation by including the electro-weak correction can decay into antiprotons [48, 55], despite the low flux. Therefore, a correlation may exist between the $e^{\pm}$ and antiproton signals induced by DM even for the leptonic annihilation channels [56]. We use PPPC [47, 48] to calculate this antiproton spectrum from DM annihilation via the e^+e^- channel and derive the corresponding $\langle\sigma v\rangle_{\bar{p}}$ limit at 95% C.L.

In Fig. 5, we show the ratios of $\langle\sigma v\rangle_{e^{\pm}}$ to $\langle\sigma v\rangle_{\bar{p}}$ with the two concentration models, considering different subhalo masses and distances. All the ratios in Fig. 5 are smaller than 1. This means that the AMS-02 antiproton measurement does not portray any excluded region. From the trends depicted in Fig. 5, we can infer that the subhalos with smaller masses and concentrations are more likely to be excluded by the antiproton observation, when explaining the tentative sharp structure in the $e^{\pm}$ spectrum. This is because such subhalos have smaller annihilation luminosities and require larger $\langle\sigma v\rangle$ accounting for the DAMPE $e^{\pm}$ spectrum, which also induces larger antiproton flux.

V. CONCLUSION

In this study, we investigate the potential impact of a nearby DM subhalo on the constraints of DM $\langle\sigma v\rangle$ inferred from the AMS-02 cosmic ray antiproton observation. We separately consider the scenarios of DM annihilation generating antiprotons with and without the nearby subhalo and present the ratios of the $\langle\sigma v\rangle$ limits for the two scenarios. For the subhalo mass ranging from $10^6M_\odot$ to $10^9M_\odot$ at a distance of 1 kpc and DM mass ranging from 30 GeV to 10 TeV, the influence of the nearby

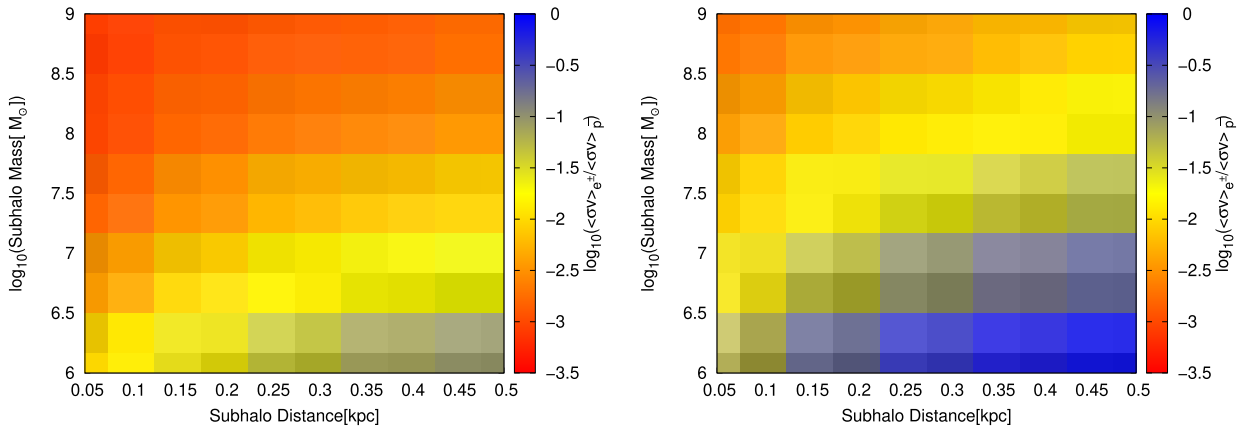

Fig. 5. (color online) The ratios of $\langle\sigma v\rangle_{e^{\pm}}$ to $\langle\sigma v\rangle_{\bar{p}}$ for DM with a mass of 1.5 TeV. $\langle\sigma v\rangle_{e^{\pm}}$ is the best fit value accounting for the tentative $e^{\pm}$ spectral structure at ~1.4 TeV reported by DAMPE. $\langle\sigma v\rangle_{\bar{p}}$ is the upper limits at 95% derived from the AMS-02 antiproton measurement for the same subhalo parameters. The left and right panels represent the concentration model 1 and 2 results, respectively.

subhalo on the $\langle\sigma v\rangle$ limits can be at most about one order of magnitude stricter than the case without the subhalo.

We explore the impact of the concentration parameter on the results. Two concentration models are employed for comparison. Since the lower concentration implies a more dispersed DM density within the subhalo, the less concentrated model is anticipated to yield a diminished effect on $\langle\sigma v\rangle$ limits. Owing to the potential enhancement of DM annihilation products caused by a wealth of subhalos in the Milky Way, we perform the previous analysis with an additional subhalo distribution. Taking the cases of 75 GeV and 1 TeV DM as examples, our results indicate that the $\langle\sigma v\rangle$ limits with the contribution from the subhalo distribution are slightly stricter than those without such contribution by a factor of $\sim 0.8-0.9$.

Finally, we apply the antiproton constraint to the DM interpretation of the tentative peak structure observed in the DAMPE cosmic ray $e^{\pm}$ spectrum at ~1.4 TeV. By fitting the DAMPE $e^{\pm}$ spectrum, we obtain the best fit $\langle\sigma v\rangle_{e^{\pm}}$ from a hypothetical nearby subhalo for various subhalo masses and distances. Simultaneously, we derive the upper limits from the antiproton measurement for the same subhalo parameters. We find that the current AMS-02 antiproton results do not set the limit on the DM interpretation accounting for the DAMPE $e^{\pm}$ spectrum at ~1.4 TeV.

References

[1] J. F. Navarro, C. S. Frenk, and S. D. M. White, Astrophys. J. **490**, 493 (1997), arXiv:astro-ph/9611107

[2] A. A. Klypin, S. Gottlober, and A. V. Kravtsov, Astrophys. J. **516**, 530 (1999), arXiv:astro-ph/9708191

[3] S. Ghigna, B. Moore, F. Governato *et al.*, Mon. Not. Roy. Astron. Soc. **300**, 146 (1998), arXiv:astro-ph/9801192

[4] A. A. Klypin, A. V. Kravtsov, O. Valenzuela *et al.*, Astrophys. J. **522**, 82 (1999), arXiv:astroph/9901240

[5] B. Moore, S. Ghigna, F. Governato *et al.*, Astrophys. J. Lett. **524**, L19 (1999)), arXiv:astro-ph/9907411

[6] C. Boehm, P. Fayet, and R. Schaeffer, Phys. Lett. B **518**, 8 (2001), arXiv:astro-ph/0012504

[7] A. M. Green, S. Hofmann, and D. J. Schwarz, Mon. Not. Roy. Astron. Soc. **353**, L23 (2004), arXiv:astroph/0309621

[8] A. M. Green, S. Hofmann, and D. J. Schwarz, JCAP **08**, 003 (2005), arXiv:astro-ph/0503387

[9] A. M. Green, S. Hofmann, and D. J. Schwarz, AIP Conf. Proc. **805**, 431 (2005), arXiv:astro-ph/0508553

[10] E. Bertschinger, Phys. Rev. D **74**, 063509 (2006), arXiv:astro-ph/0607319

[11] V. Berezinsky, V. Dokuchaev, and Y. Eroshenko, Phys. Rev. D **77**, 083519 (2008), arXiv:0712.3499[astro-ph]

[12] J. Diemand, M. Kuhlen, and P. Madau, Astrophys. J. **667**, 859 (2007), arXiv:astro-ph/0703337

[13] A. Loeb and M. Zaldarriaga, Phys. Rev. D **71**, 103520 (2005), arXiv:astro-ph/0504112

[14] J. Diemand, B. Moore, and J. Stadel, Nature **433**, 389 (2005), arXiv:astro-ph/0501589

[15] L. Gao, S. D. M. White, A. Jenkins *et al.*, Mon. Not. Roy. Astron. Soc. **363**, 379 (2005), arXiv:astro-ph/0503003

[16] J. Diemand, M. Kuhlen, and P. Madau, Astrophys. J. **649**, 1 (2006), arXiv:astro-ph/0603250

[17] V. Springel, S. D. M. White, G. Tormen *et al.*, Mon. Not. Roy. Astron. Soc. **328**, 726 (2001), arXiv:astro-ph/0012055

[18] A. R. Zentner and J. S. Bullock, Astrophys. J. **598**, 49 (2003), arXiv:astro-ph/0304292

[19] G. Tormen, A. Diaferio, and D. Syer, Mon. Not. Roy. Astron. Soc. **299**, 728 (1998), arXiv:astro-ph/9712222

[20] S. Ghigna, B. Moore, F. Governato *et al.*, Astrophys. J. **544**, 616 (2000), arXiv:astro-ph/9910166

[21] C. D. Wilson *et al.*, Mon. Not. Roy. Astron. Soc. **424**, 3050 (2012), arXiv:1206.1629[astro-ph.CO]

[22] G. De Lucia, G. Kauffmann, V. Springel *et al.*, Mon. Not. Roy. Astron. Soc. **348**, 333 (2004), arXiv:astroph/0306205

[23] A. V. Kravtsov, O. Y. Gnedin, and A. A. Klypin, Astrophys. J. **609**, 482 (2004), arXiv:astro-ph/0401088

[24] G. Kauffmann, S. D. M. White, and B. Guiderdoni, Mon. Not. Roy. Astron. Soc. **264**, 201 (1993)
[25] L. Gao, S. D. M. White, A. Jenkins *et al.*, Mon. Not. Roy. Astron. Soc. **355**, 819 (2004), arXiv:astro-ph/0404589
[26] V. Springel, J. Wang, M. Vogelsberger *et al.*, Mon. Not. Roy. Astron. Soc. **391**, 1685 (2008), arXiv:0809.0898[astro-ph]
[27] J. Diemand, M. Kuhlen, P. Madau *et al.*, Nature **454**, 735 (2008), arXiv:0805.1244[astro-ph]
[28] S. Garrison-Kimmel, M. Boylan-Kolchin, J. Bullock *et al.*, Mon. Not. Roy. Astron. Soc. **438**, 2578 (2014), arXiv:1310.6746[astro-ph.CO]
[29] A. Cuoco, M. Krämer, and M. Korsmeier, Phys. Rev. Lett. **118**, 191102 (2017), arXiv:1610.03071[astroph.HE]
[30] M.-Y. Cui, Q. Yuan, Y.-L. S. Tsai *et al.*, Phys. Rev. Lett. **118**, 191101 (2017), arXiv:1610.03840[astroph.HE]
[31] M.-Y. Cui, X. Pan, Q. Yuan *et al.*, JCAP **06**, 024 (2018), arXiv:1803.02163[astro-ph.HE]
[32] A. Cuoco, J. Heisig, L. Klamt *et al.*, Phys. Rev. D **99**, 103014 (2019), arXiv:1903.01472[astro-ph.HE]
[33] I. Cholis, T. Linden, and D. Hooper, Phys. Rev. D **99**, 103026 (2019), arXiv:1903.02549[astro-ph.HE]
[34] S.-J. Lin, X.-J. Bi, and P.-F. Yin, Phys. Rev. D **100**, 103014 (2019), arXiv:1903.09545[astro-ph.HE]
[35] M. Boudaud, Y. Génolini, L. Derome *et al.*, Phys. Rev. Res. **2**, 023022 (2020), arXiv:1906.07119[astro-ph.HE]
[36] J. Heisig, M. Korsmeier, and M. W. Winkler, Phys. Rev. Res. **2**, 043017 (2020), arXiv:2005.04237[astro-ph.HE]
[37] F. Kahlhoefer, M. Korsmeier, M. Krämer *et al.*, JCAP **12**, 037 (2021), arXiv:2107.12395[astro-ph.HE]
[38] C.-R. Zhu, M.-Y. Cui, Z.-Q. Xia *et al.*, Phys. Rev. Lett. **129**, 231101 (2022), arXiv:2204.03767[astro-ph.HE]
[39] X.-J. Lv, X.-J. Bi, K. Fang *et al.*, (2023), arXiv:2304.00760[astro-ph.HE]
[40] M. Aguilar *et al.* (AMS), Phys. Rept. **894**, 1 (2021)
[41] J. Chang *et al.* (DAMPE), Astropart. Phys. **95**, 6 (2017), arXiv:1706.08453[astro-ph.IM]
[42] I. V. Moskalenko and A. W. Strong, Astrophys. J. **493**, 694 (1998), arXiv:astro-ph/9710124
[43] A. W. Strong and I. V. Moskalenko, Astrophys. J. **509**, 212 (1998), arXiv:astro-ph/9807150
[44] T. K. Gaisser, R. Engel, and E. Resconi, *Cosmic Rays and Particle Physics: 2nd Edition* (Cambridge University Press, 2016).
[45] Q. Yuan, S.-J. Lin, K. Fang *et al.*, Phys. Rev. D **95**, 083007 (2017), arXiv:1701.06149[astro-ph.HE]
[46] M. di Mauro, F. Donato, A. Goudelis *et al.*, Phys. Rev. D **90**, 085017 (2014) [Erratum: Phys. Rev. D **98**, 049901 (2018)], arXiv: 1408.0288[hep-ph]
[47] M. Cirelli, G. Corcella, A. Hektor *et al.*, JCAP **03**, 051 (2011) [Erratum: JCAP **10**, E01 (2012)], arXiv: 1012.4515[hep-ph].
[48] P. Ciafaloni, D. Comelli, A. Riotto *et al.*, JCAP **03**, 019 (2011), arXiv:1009.0224[hep-ph]
[49] Q. Yuan *et al.*, (2017), arXiv: 1711.10989[astro-ph.HE]
[50] P. Brun, T. Delahaye, J. Diemand *et al.*, Phys. Rev. D **80**, 035023 (2009), arXiv:0904.0812[astro-ph.HE]
[51] A. V. Maccio', A. A. Dutton, and F. C. v. d. Bosch, Mon. Not. Roy. Astron. Soc. **391**, 1940 (2008), arXiv:0805.1926[astro-ph]
[52] M. Kamionkowski, S. M. Koushiappas, and M. Kuhlen, Phys. Rev. D **81**, 043532 (2010), arXiv:1001.3144[astroph.GA]
[53] M. Kamionkowski and S. M. Koushiappas, Phys. Rev. D **77**, 103509 (2008), arXiv:0801.3269[astro-ph]
[54] G. Ambrosi *et al.* (DAMPE), Nature **552**, 63 (2017), arXiv:1711.10981[astro-ph.HE]
[55] P. Ciafaloni, M. Cirelli, D. Comelli *et al.*, JCAP **06**, 018 (2011), arXiv:1104.2996[hep-ph]
[56] A. De Simone, A. Riotto, and W. Xue, JCAP **05**, 003 (2013), arXiv:1304.1336[hep-ph]